JKAS
Journal of the Korean Astronomical Society
http://jkas.kas.org
eISSN: 2288-890X · pISSN: 1225-4614
JKAS (2023), **56**, 2, 225–229
doi: 10.5303/JKAS.2023.56.2.225

Dynamic Formation and Associated Heating of a Magnetic Loop on the Sun. II. A Characteristic of an Emerging Magnetic Loop with the Effective Footpoint Heating Source

Tetsuya Magara[1,2,*], **Yeonwoo Jang**[2], **and Donghui Son**[2]

[1]Department of Astronomy and Space Science, Kyung Hee University, Yongin-si, Gyeonggi-do 17104, Republic of Korea
[2]School of Space Research, Kyung Hee University, Yongin-si, Gyeonggi-do 17104, Republic of Korea
*Corresponding Author: T. Magara, magara@khu.ac.kr

Received September 19, 2023; Accepted November 14, 2023; Published November 24, 2023

Abstract

We investigated an emerging magnetic loop dynamically formed on the Sun, which has the effective footpoint heating source that may play a key role in heating a solar atmosphere with free magnetic energy in it. It is suggested that the heating source could be related to local compression of a plasma in the emerging loop by means of Lorentz force, which converts the magnetic energy to the internal energy of the plasma that is used to reaccelerate a decelerated downflow along the loop, eventually generating the source when the kinetic energy of the downflow is thermalized. By analyzing very high-cadense data obtained from a magnetohydrodynamic simulation, we demonstrate how the local compression is activated to trigger the generation of the heating source. This reveals a characteristic of the emerging loop that experiences a dynamic loop-loop interaction, which causes the local compression and makes the plasma gain the internal energy converted from the magnetic energy in the atmosphere. What determines the characteristic that could distinguish an illuminated emerging loop from a nonilluminated one is discussed.

Keywords: Sun: atmosphere — Sun: magnetic fields — magnetohydrodynamics — methods: numerical

1. Introduction

The Sun has a magnetized atmosphere where subsurface magnetic flux continuously emerges by the magnetic buoyancy (Parker 1955) to form a number of emerging magnetic loops, known as flux emergence. Lorentz force tends to expand them, meaning that the solar magnetized atmosphere contains free magnetic energy. On the other hand, a significant heating proceeds in the atmosphere to illuminate those emerging loops selectively and intermittently, and its source and mechanism have intensively been studied (Parker 1972; Heyvaerts & Schatzman 1980; Hollweg 1981; Sturrock & Uchida 1981; van Ballegooijen 1986; Parker 1988; Low 1990; Ofman et al. 1994; Inverarity & Priest 1995; Galsgaard & Nordlund 1996; Belien et al. 1999; Matthaeus et al. 1999; Cranmer & van Ballegooijen 2005; Aschwanden 2005 and references therein; Kittinaradorn et al. 2009; Goossens et al. 2011; Reale 2014 and references therein; Howson et al. 2019). Recently, we proposed a possible mechanism of the solar atmospheric heating that cooperates with dynamic formation of a selected emerging loop via the flux emergence (Magara et al. 2022, hereafter Paper I). In this mechanism the effective footpoint heating source (eFHS) generated in the selected loop plays a key role. In Paper I we report a result showing what dynamic and thermodynamic states of a plasma in that loop are involved in the generation of the eFHS.

The result, when we derive characteristics of emerging loops where the eFHS is generated (hereafter, eFHS-loops), could lead to understanding how an illuminated emerging loop is formed in the solar magnetized atmosphere. Since dynamic and thermodynamic states continuously change inside each emerging loop as the flux emergence proceeds, the evolution of eFHS-loops should be investigated in order to see what the characteristics are and how they are acquired by these loops. In Paper I we identify one such loop from a magnetohydrodynamic (MHD) simulation reported in Magara (2017), and clarify the dynamic and thermodynamic states observed when the eFHS is generated in this loop, although how these states are established remains unclear.

As a follow-up study, we used the MHD simulation to make a further investigation focused on the evolutionary path leading to an eFHS-loop. This revealed a characteristic represented by a triggering process for the eFHS, which was derived by analyzing very high-cadense simulated data, as explained below.

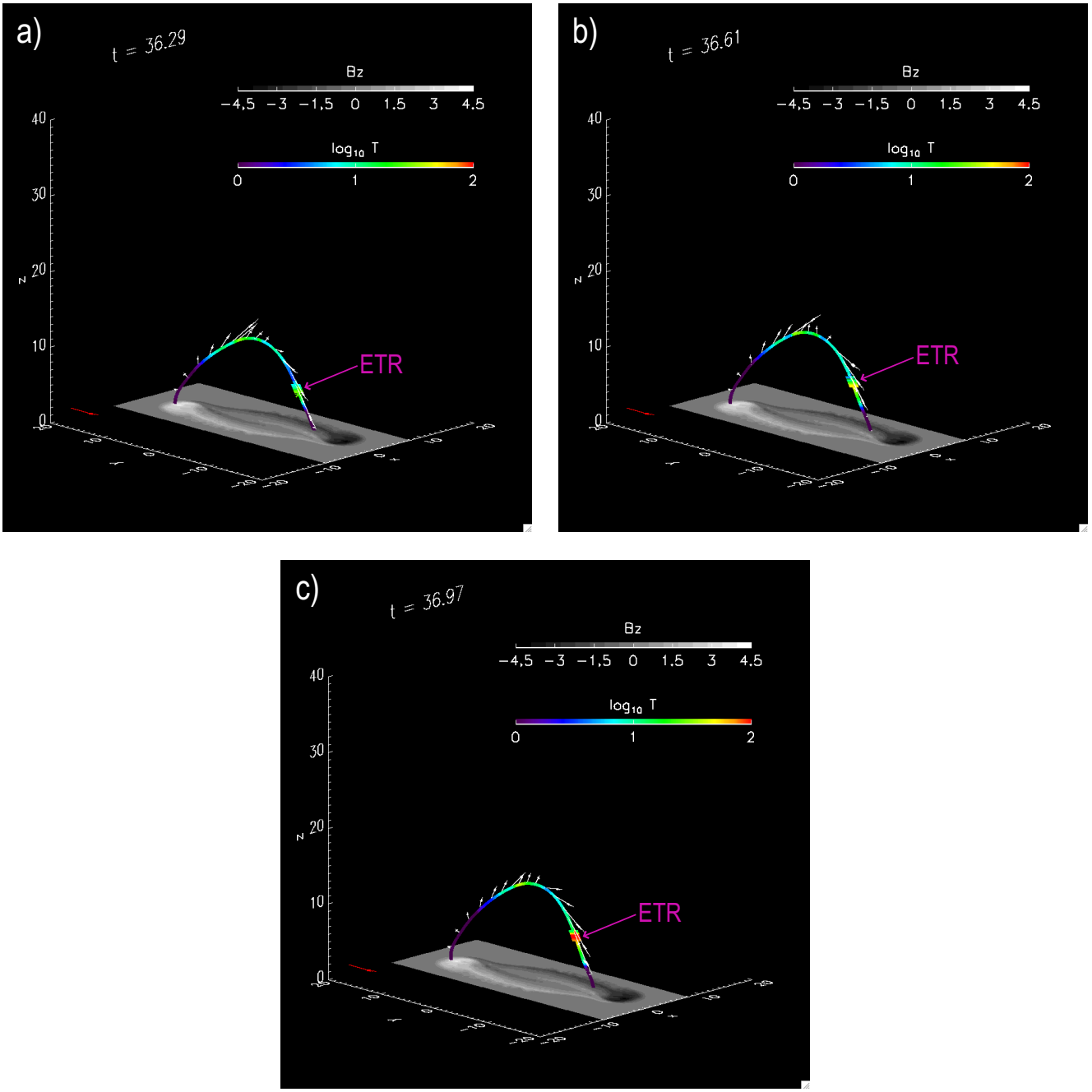

Figure 1. a-c: Snapshots of eFHS-loop identified from the MHD simulation, taken at $t = 36.29$ (a), 36.61 (b), 36.97 (c). Field-line colors and arrows represent temperature and flow velocity distributed along the loop, while gray-scale contour map at $z = 0$ the distribution of photospheric magnetic flux density. The length of red arrow at bottom-left corner corresponds to a speed of 10. Enhanced temperature region (ETR) is indicated by thick field line segment in each panel. Normalization units are given by $2H_{ph}$ (length), c_{ph} (velocity), ρ_{ph} (gas density), $\rho_{ph}c_{ph}^2$ (gas pressure), T_{ph} (temperature), and $(\rho_{ph}c_{ph}^2)^{1/2}$ (magnetic field), where H_{ph}, c_{ph}, ρ_{ph}, and T_{ph} are the pressure scale height, adiabatic sound speed, gas density, and temperature at the photosphere. We adopted $\gamma = 5/3$ and $\mu = 0.6$ as the specific heat ratio and mean molecular weight, respectively, so $2H_{ph} = 540$ km in the simulation. A movie is provided (http://163.180.179.74/~magara/Download/JKAS2023/fig1.mp4).

2. Simulated Data & Result

First let us briefly overview the generation process of the eFHS discussed in Paper I. While evolving in a low plasma β atmosphere such as the solar magnetized atmosphere, a selected emerging loop is subjected to local compression by the magnetic field surrounding that loop, in which a strong supersonic downflow is produced to form a shock wave and generate the eFHS. A key issue in this process is to demonstrate how to activate the local compression of a plasma in the cross-section direction of the selected loop (hereafter, $\perp$-direction) by means of Lorentz force, which converts the magnetic energy in the atmosphere to the internal energy of the plasma. To clarify this issue, we identified an eFHS-loop from the MHD simulation and investigated the evolution of this loop by following its Lagrangian displacement. The eFHS appears rather abruptly between $t = 36.8$ and 37.0 in the identified loop, suggesting that emergent activation may occur around this short period

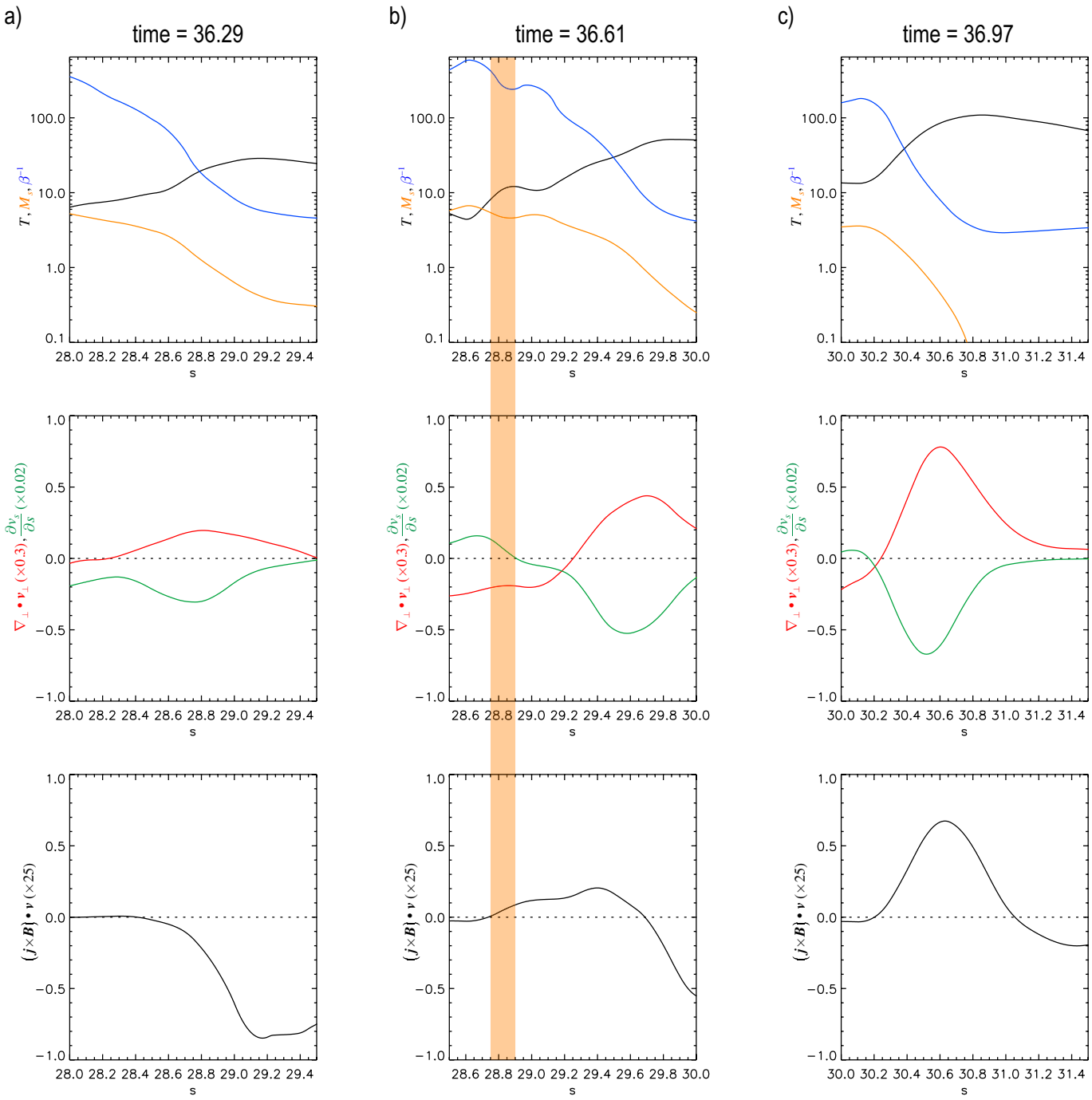

Figure 2. a-c: Three graphs accompanying each panel in Figure 1 are presented, showing distributions of temperature (top, multiplied by 1, black curve), Mach number of v_s (top, multiplied by 1, orange curve), inverse of plasma beta (top, multiplied by 1, blue curve), $\nabla_\perp \cdot \mathbf{v}_\perp$ [middle, multiplied by 0.3, red curve, derived from Eq. (1)], $\partial v_s/\partial s$ (middle, multiplied by 0.02, green curve), $\mathbf{j} \times \mathbf{B} \cdot \mathbf{v}$ (bottom, multiplied by 25) in ETR. The range of the graphs relevant to local compression by means of Lorentz force associated with local expansion along the loop is highlighted in orange.

in an upstream region close to the appearance position of the eFHS, during which dynamic and thermodynamic states barely change in other distant portions of the loop. To catch the moment when the above-mentioned local compression occurs in the upstream region, we analyzed the very high-cadence simulated data obtained at a time interval of $\Delta t = 0.01$, compared to $\Delta t = 0.2$ in Paper I and $\Delta t = 1$ in Magara (2017).

Figure 1 presents snapshots of the identified loop taken at $t = 36.29$ (panel a), 36.61 (panel b), 36.97 (panel c), where the field-line colors and arrows represent the temperature and flow velocity distributed along the loop, respectively, while the gray-scale contour map at $z = 0$ the distribution of photospheric magnetic flux density. Each panel is accompanied by the three graphs presented in Figure 2, showing how the temperature T, Mach number of a downflow along the loop M_s, inverse of plasma beta β^{-1} (top), $\nabla_\perp \cdot \mathbf{v}_\perp$, $\partial v_s/\partial s$ (middle), $\mathbf{j} \times \mathbf{B} \cdot \mathbf{v}$ (bottom) are distributed in the enhanced temperature region (ETR) indicated by the thick field line segment in the panel.

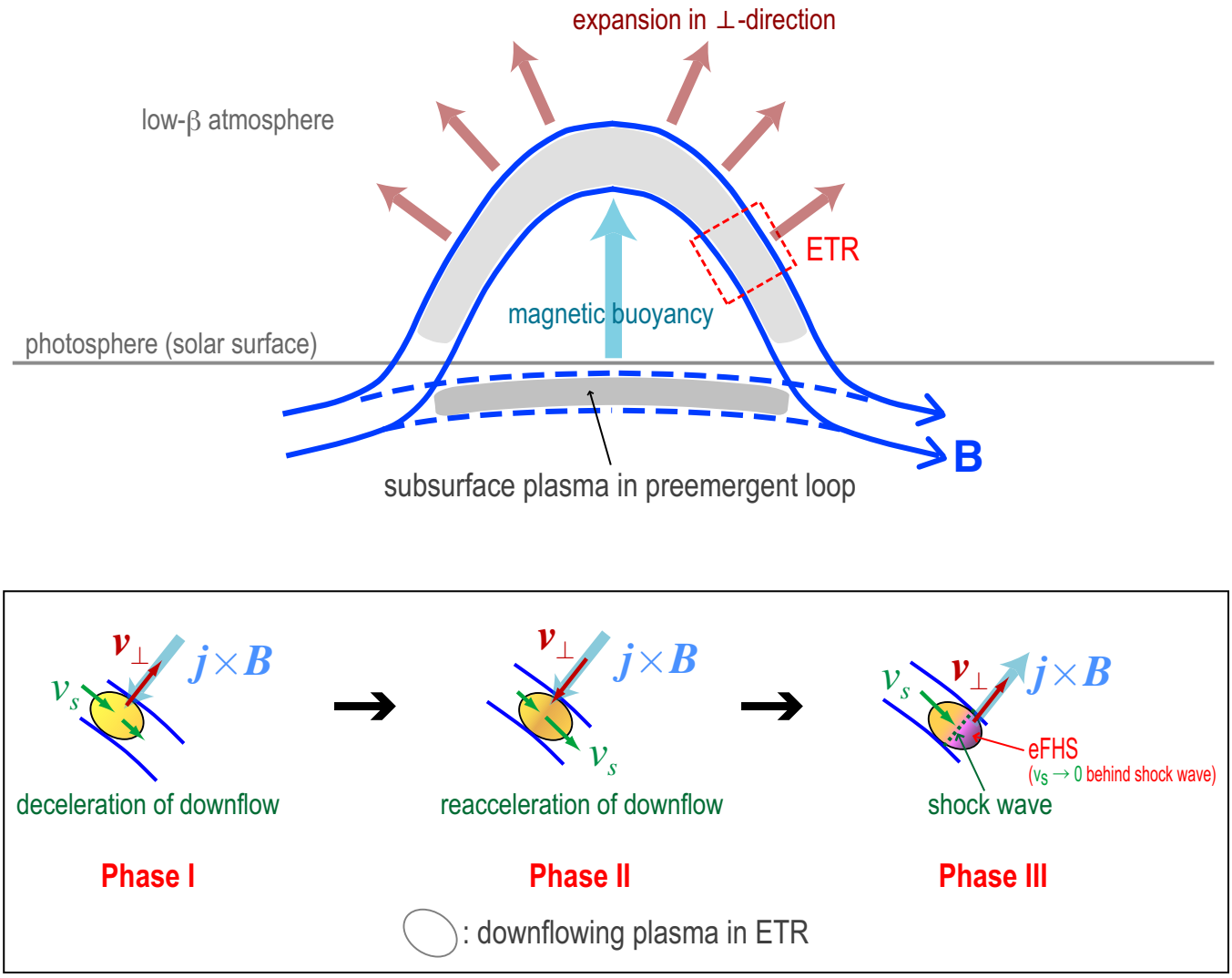

Figure 3. Schematic illustration of eFHS-loop. At Phase II a small rate of change in the magnetic energy density ϵ_m tends to cause a large rate of change in the internal energy density of plasma ϵ_p via energy conversion in low-β atmosphere ($\Delta\epsilon_p/\epsilon_p \sim \beta^{-1}\Delta\epsilon_m/\epsilon_m$). At Phase III the deceleration of downflow associated with strong compression along the loop further proceeds behind the shock wave, reducing v_s efficiently (Paper I). Colors of downflowing plasma in ETR represent variations in temperature shown by Figure 2. For other details, see the text.

Here $\nabla_\perp \cdot \mathbf{v}_\perp$, local expansion/compression rate in the $\perp$-direction, is given by

$$\nabla_\perp \cdot \mathbf{v}_\perp = \nabla \cdot \mathbf{v} - \frac{\partial v_s}{\partial s}, \tag{1}$$

where s is a curved coordinate variable along the loop, representing the length measured from its photospheric footpoint with positive magnetic polarity. At $t = 36.29$ the downflow is decelerated along the loop via compression of a downflowing plasma in the s-direction ($\partial v_s/\partial s < 0$), while compression of the plasma in the $\perp$-direction is hardly observed in the ETR. This is normal because Lorentz force tends to expand emerging loops. Interestingly, Lorentz force at that time does negative work there, suggesting that the force tries to change the dynamic state of the plasma locally from expansion to compression in the $\perp$-direction. At $t = 36.61$ it is found that the plasma is compressed in the $\perp$-direction at a portion of the loop, where Lorentz force does positive work to convert the magnetic energy to the internal energy of the plasma, as indicated by a local hump in the temperature plot (see the range highlighted in orange). This enhances the gas pressure locally, reaccelerating the decelerated downflow via expansion of the plasma in the s-direction (see $\partial v_s/\partial s > 0$ in the highlighted range). At $t = 36.97$ the maximum temperature in the ETR reaches a value of more than 100, which is caused by the strong compression of the plasma in the s-direction that converts almost all the kinetic energy of the downflow to heat, as explained in Paper I. The compressed plasma, on the other hand, expands in the $\perp$-direction, facilitated by Lorentz force doing positive work.

3. Summary & Discussion

It is worth mentioning two basic properties of emerging loops in the solar magnetized atmosphere. One of them is that these loops are not isolated; that is, each emerging loop always has neighbors even if they are not illuminated, because the magnetic field emerging to the atmosphere is continuously distributed there. The other property is that each emerging

loop basically has its own dynamic profile to evolve differently from one another in the atmosphere.

These two properties lead us to expect that a loop-loop interaction tends to occur between emerging loops, and the interaction may be classified into two types; purely dynamic (frozen-in) type and diffusive (non-frozen-in) type. The first type indicates that the interaction is conducted in a purely dynamic way, not affecting the integrity of each interacting loop. The second type potentially involves a topological change in magnetic field lines that could destroy the magnetic structure of each interacting loop. Obviously, what we discuss here is related to the first type, purely dynamic loop-loop interaction preserving the magnetic loop integrity.

Figure 3 summarizes the characteristic of the eFHS-loop derived from this study. Through the purely dynamic loop-loop interaction the magnetic pressure at the interface between the eFHS-loop and the other interacting loop is temporarily enhanced, which facilitates the downflowing plasma in the eFHS-loop to change the dynamic state from expansion to compression in the $\perp$-direction (Phase I). Lorentz force then does positive work on the plasma, increasing the internal energy via the magnetic compression that causes the local enhancement of the gas pressure, reaccelerating the decelerated downflow along the loop (Phase II). The kinetic energy of the downflow is eventually thermalized to generate the eFHS (Phase III).

Energetically, the main energy of the eFHS may come from the kinetic energy of the downflow developed in the eFHS-loop. The magnetic compression at Phase II only provides part of this energy because even though it is decelerated before the reacceleration, the downflow is mostly supersonic in the upstream region at Phase I (see Figure 2a), while at Phase III the speed of the downflow rapidly decreases and most of its kinetic energy is thermalized to generate the eFHS. This suggests that a rigid wall-like region is formed inside the loop between Phase I and Phase III. The reacceleration caused by the magnetic compression may contribute little to the energy of the eFHS, but could work as a trigger for the formation because it will transport more mass to the downstream region in a short time, making that region 'more rigid' and forming the shock wave in front of it.

What matters is the characteristic represented by a transition from Phase I to Phase III through Phase II, and the magnetic compression plays a key role in the transition. This result was derived from the very high-cadense data obtained by reperforming the MHD simulation with a new set of Lagrangian tracers, and using the data we are enabled to demonstrate what physical process is activated in the nearby upstream region of the eFHS just before its abrupt appearance.

We may ask about how heat is transferred from the eFHS to the other portions of the eFHS-loop, thereby illuminating it. We expect that thermal conduction plays the central role in redistributing the heat, which will be investigated by performing a separate simulation where the conduction is incorporated.

Generally, a plasma in emerging loops loses the internal energy via expansion and radiation in the solar magnetized atmosphere. If a selected emerging loop experiences the dynamic loop-loop interaction 'multiple times', the plasma in that loop could gain a significant amount of the internal energy converted from the magnetic energy in the atmosphere. An interesting question is then whether this determines the characteristic that could distinguish an illuminated emerging loop from a nonilluminated one. Here we assume that the former is more subjected to the magnetic compression than the latter so that the internal energy accumulated in the former through multiple times of the interaction is sufficient to generate the eFHS with a temperature that is dependent on the number of occurrence and magnitude of the interaction. To answer the question, more long-term evolution of the eFHS-loop specified by its Lagrangian displacement than that presented in this paper, especially the evolution before Phase I, should be investigated. This is the target of our forthcoming research.

Acknowledgments

The authors deeply appreciate valuable comments provided by the referee. They wish to thank the Kyung Hee University for general support of this work. This work was financially supported by a research program (NRF-2021R1A2C1010310, PI: T. M.) through the National Research Foundation of Korea (NRF) funded by the Ministry of Education, Science and Technology.

References

Aschwanden, M. J. 2005, Physics of the Solar Corona. An Introduction with Problems and Solutions, 2nd edn. (New York, Berlin: Springer)

Belien, A. J. C., Martens, P. C. H., & Keppens, R. 1999, in ESA Special Publication, Vol. 446, 8th SOHO Workshop: Plasma Dynamics and Diagnostics in the Solar Transition Region and Corona, ed. J. C. Vial & B. Kaldeich-Schü, 167

Cranmer, S. R., & van Ballegooijen, A. A. 2005, ApJS, 156, 265

Galsgaard, K., & Nordlund, Å. 1996, J. Geophys. Res., 101, 13445

Goossens, M., Erdélyi, R., & Ruderman, M. S. 2011, Space Sci. Rev., 158, 289

Heyvaerts, J., & Schatzman, E. 1980, in Japan-France Seminar on Solar Physics, ed. F. Moriyama & J. C. Henoux, 77

Hollweg, J. V. 1981, Sol. Phys., 70, 25

Howson, T. A., De Moortel, I., Reid, J., & Hood, A. W. 2019, A&A, 629, A60

Inverarity, G. W., & Priest, E. R. 1995, A&A, 302, 567

Kittinaradorn, R., Ruffolo, D., & Matthaeus, W. H. 2009, ApJ, 702, L138

Low, B. C. 1990, ARA&A, 28, 491

Magara, T. 2017, PASJ, 69, 5

Magara, T., Jang, Y., & Son, D. 2022, JKAS, 55, 215 [Paper I]

Matthaeus, W. H., Zank, G. P., Oughton, S., Mullan, D. J., & Dmitruk, P. 1999, ApJ, 523, L93

Ofman, L., Davila, J. M., & Steinolfson, R. S. 1994, ApJ, 421, 360

Parker, E. N. 1955, ApJ, 121, 491

Parker, E. N. 1972, ApJ, 174, 499

Parker, E. N. 1988, in Solar and Stellar Coronal Structure and Dynamics, ed. R. C. Altrock, 2–17

Reale, F. 2014, Living Rev. Sol. Phys., 11, 4

Sturrock, P. A., & Uchida, Y. 1981, ApJ, 246, 331

van Ballegooijen, A. A. 1986, ApJ, 311, 1001